NASA Technical Paper 3327

January 1993

Hypersonic Rarefied Wake Characterization

E. B. Brewer

NASA

Hypersonic Rarefied Wake Characterization

E. B. Brewer
*George C. Marshall Space Flight Center
Marshall Space Flight Center, Alabama*

TABLE OF CONTENTS

LIST OF ILLUSTRATIONS

LIST OF TABLES

NOMENCLATURE

C_f	skin friction coefficient, $C_f = 2\tau_w/(\rho V^2)_\infty$
C_p	pressure coefficient, $C_p = 2p/(\rho V^2)_\infty$
d	diameter of sphere
D	molecular diameter
Kn	Knudsen number, $Kn = \lambda/d$
M	Mach number
M	molecular weight
p	pressure
q_{ref}	$(\rho V^3)_\infty/2$
Re_o	Reynolds number, $Re = \rho V d/\mu_o$
S	speed ratio, $S = V/(2RT)^{0.5}$
T	thermodynamic temperature
T_w	surface temperature
V	freestream velocity
χ_i	mole fraction of species i
x	distance from sphere center measured parallel to freestream
y	radial distance from axis of symmetry
λ	mean free path
μ	dynamic viscosity
ρ	density
τ	shear stress
ω	temperature exponent of the coefficient of viscosity

Subscripts

i	ith species
w	surface values
o	freestream total values
∞	freestream static values

Abbreviations

AFE	aeroassist flight experiment
ASTV	aeroassisted space transfer vehicle
VHS	variable hard sphere
NAS	numerical aerodynamic simulation facility

-

TECHNICAL PAPER

HYPERSONIC RAREFIED WAKE CHARACTERIZATION

INTRODUCTION

Due to the aeroassist flight experiment (AFE), there has been a renewed interest in rarefied hypersonic flight after a considerable period of dormancy. The AFE program, which is now on hold, was a mission to obtain science data at rarefied flow conditions not available to the aerothermodynamicist in wind tunnels. Those science data are needed to confidently design an aeroassisted space transfer vehicle (ASTV).

An ASTV will consist of an aerobrake, a payload, and a propulsion unit. The aerobrake protects the payload from the severe aerothermodynamic environment of hypersonic entry into the atmosphere. However, the environment of the payload which resides in the wake of the aerobrake still must be defined. Little is known about these wakes. It is the purpose of this paper to characterize the rarefied hypersonic wake and its interaction with a payload. This basic information will be useful in designing the aerobrake and its payload and for understanding the tethered satellite wake.

COMPUTATIONAL METHOD

The direct simulation Monte Carlo (DSMC) method[1-3] is the only method presently available to handle rarefied wake flow. The five-specie air chemistry model[4] was used in these calculations. The 11-specie model, which includes the five species O_2, O, N_2, N, NO and their ions along with the electron, is appropriate for these reentry conditions, but lacks the maturity of the five-specie model. It is hoped that the ionization which will occur will have little influence on the structure of the wake. Dr. Bird's two-dimensional or axisymmetric code[5] was used for the axisymmetric calculations. An equivalent code written by the author was used for the three-dimensional AFE calculations.

RESULTS AND DISCUSSION

While the capabilities and accuracy of the DSMC method are quite well documented, benchmark calculations are still necessary to add to the experience base when it is used to predict results for new problems or different geometries. While Dogra et al.[7] looked at hypersonic rarefied flow past spheres, including the wake structure, the results were compared only with the drag force from Legge and Koppenwallner's experiment.[8]

Sphere Wake Flow Benchmark

Muthoo and Brundin[6] presented, at the RGD symposium in Gottingen, near wake measurements of a sphere at M = 5.6 and Kn = 0.005 run in the Oxford University low-density wind tunnel. These data

were used as a benchmark case in order to further validate the code for this study. A cold gas model used $T_{ref} = 300$ K and viscosity exponent $\omega = 0.91$ rather than $\omega = 0.75$ which is normally used for air at normal temperatures because of the very cold freestream temperature of the Oxford tunnel.

The DSMC results are given in figures 1 through 3. Contour plots of density, velocity, and temperature are shown in figure 1. The wake density field from both analysis and experiment indicated a broad recompression region and weak trailing shock or recompression fan. There is no recirculation in the base region as indicated by the vector plot given in figure 2. Experiment and DSMC are in excellent agreement with respect to the defects of velocity and density along the wake centerline beyond an x/d of one as shown in figure 3. The translational kinetic temperature was calculated from the collection of molecules in each cell, and the pressure was calculated from the equation of state in order to compare with the experimental data. For regions of nonequilibrium, the thermodynamic temperature and the translational temperature will not be equal. Both analysis and experiment (fig. 3) show that there is no separation in the wake; however, in their paper, Muthoo and Bruden state that rear stagnation point is located approximately at $x/d = 1.5$ where the axial static pressure is a maximum. The DSMC results indicate that the maximum static pressure occurs near an $x/d = 1.25$; however, an interpretation that this is a stagnation point is not correct. This is a characteristic of rarefied wakes, and more will be said later. Obviously, experiment and analysis agree, as is shown in figure 3, as to the velocity distribution in the wake, and there is no flow reversal.

The differences between the DSMC results and experiment in the near wake might be attributed to experimental error due to the large mean free path in that region of the flow. The physical size of the instrumentation, the low-density corrections required on their response, and probe interference with the flow probably significantly affect the experimental results in close proximity to the sphere. The flow in this region is not in equilibrium and with the rarefaction the continuum concepts of temperature and pressure become invalid. Density remains the significant flow property, but the experimental value was not measured directly, of course. It is a result of analysis of hot wire and pressure data. Even today, it would be very difficult to make meaningful measurements in the very near wake of a sphere.

Sphere Wake Flow Characterization

The surface shear stress near the sphere aft stagnation point indicates that the flow may be nearing separation for the benchmark flow conditions. Using the same grid, the calculations were pushed to higher Reynolds numbers until flow separation occurred. Further increases in Reynolds number then increased the extent of the separation zone. Several cases were run at various Reynolds numbers and Mach numbers as indicated in tables 1, 2, and 3. Typical $T_w/T_o = 1$ results are plotted in figures 4 and 5 for Re_o greater than 600. The calculations at the highest Reynolds numbers are certainly coarse grid results near the windward stagnation point, but on the wake side the grid is adequate relative to the local mean free path. However, near the sphere, the steep gradients indicate that a finer grid is desirable. In any case, the extent of the predicted flow separation is given in figure 6 as a function of the Reynolds number with viscosity evaluated at the flow total temperature, Re_o. The value of $Re_o = 600$ corresponds approximately to incipient separation for a $T_w/T_o = 1$ for M = 5.6 and M = 30 as well, exhibiting some degree of Mach number independence.

For a cold wall, one would expect separation to occur at lower Reynolds numbers, and that is what happens as shown in figure 6. Typical $T_w/T_o = 0.1$ results are plotted in figures 7 and 8. While the data shown for the M = 30 case are insufficient to determine the separation Reynolds number, it appears that Mach number independence does extend to the cold wall case.

2

ASTV Configuration

Since there are expected to be configuration effects upon the wake flow, a geometry more representative of an ASTV than a sphere has been considered. An ASTV will consist of an aerobrake and a payload. The configuration used here is a hemispherical aerobrake with a cylindrical payload for simplicity. The radius of the payload was arbitrarily set at half the radius of the hemisphere. The front surface of the aerobrake was set to 1,000 K, while the aft aerobrake surface and the payload were set to 300 K.

The freestream velocity was set at 10 km/s. The ambient conditions used correspond approximately to the altitudes of 86, 92, 100, and 110 km and were taken from the 1972 Standard Atmosphere. Since the hemisphere diameter is 1.0 m, the Knudsen number is equal to the mean free path. The freestream conditions are given in tables 4 and 5.

For all the cases run over the transitional flow regime, the near wake was separated near the hemisphere. This is a marked contrast to the sphere results where the wake is not separated in the transitional flow regime. In fact, when molecular collisions were suppressed, i.e., collisionless flow, the wake still exhibited a separated flow streamline pattern. A representative wake flow field is shown in figures 9 and 10 where density, velocity, and temperature contours are plotted.

One might expect the flow over a hemisphere to separate at a lower Reynolds number relative to a sphere, but its persistence to free molecular flow indicates that the payload or afterbody must also be having an effect. One could eliminate the payload from the geometry to determine its effect; however, its effect can be eliminated by applying a plane of symmetry boundary condition at its surface. There is then no heat transfer or skin friction at the payload surface either. Thus, applying a specular reflecting boundary condition at the payload surface gives the advantage of keeping the same computational space and grid as before while eliminating the effects of the payload. Further, starting with the diffuse boundary condition results, the new results are obtained quickly.

The results are given in figures 11 and 12. The wake is now unseparated (except at the lowest Knudsen number) in conformity with the sphere results. A comparison of the streamlines for the two cases is shown in figure 13. The location of the stagnation point on the payload is quite close to the aerobrake. In contrast to high Reynolds number flows, where this point is usually associated with high heating, the thermal environment at this point in the rarefied wake is quite benign.

The heating, pressure, and skin friction distributions along the payload are shown in figures 14, 15, and 16, respectively, for selected Knudsen numbers. The surface pressure peaks at a slightly lower x/d (0.6 to 0.8) value in comparison to the heating rate and shear stress (0.8 to 1.0). The heating at the stagnation point on the payload ($x/d < 0.15$) is an order or so less than the maximum.

AFE Configuration

An ASTV will be a lifting body and will have a three-dimensional wake like the AFE configuration. The AFE payload is the carrier vehicle. The DSMC method was used previously to determine the wake flow characteristics of the AFE.[9] The wake results were a little puzzling, and one always questions the validity of first results. The AFE and its wake are three-dimensional and require a great deal of computer time and memory. The grid resolution is never as good as one would like with the computer resources being the constraint. In this case, the computations were done on the best facilities available, being the NAS facility at Ames Research Center.

Shown in figure 17 are the flow vectors obtained in the plane of symmetry of the AFE wake at an altitude of 100 km and a velocity of about 9.9 km/s. The flow separates from the aerobrake and impinges on the carrier vehicle (the afterbody or payload) near the upper part of the figure. Recirculation appears near the carrier vehicle in the lower part of the figure. The wake behind the afterbody is not separated. These wake characteristics were the same at all altitudes calculated from 95 to 120 km (Knudsen range from 0.03 to 0.8). This wake behavior is consistent with and now explainable by the ASTV results presented in the previous section of this report.

CONCLUSIONS

The wake flow field has been calculated using DSMC for hot and cold spheres at freestream conditions near continuum. Separation on nearly adiabatic spheres has been predicted to occur near a postshock Reynolds number of 600 and for cold spheres near 100. For more rarefied conditions, the wake does not separate. It has been shown that an afterbody or payload in the wake of a hemispherical aerobrake will cause the near wake flow to separate over the whole transitional flow range from continuum to free molecular flow. This is in sharp contrast to aerobrakes without afterbodies where the flow is generally not separated except in the near continuum. For a short, blunt-based afterbody like the carrier vehicle in the wake of the AFE aerobrake, separation occurs over the afterbody, while the wake behind the afterbody (carrier vehicle) is not separated.

No matter how short the afterbody, the flow will be separated near the aerobrake end of the payload. However, the heating, shear stress, and pressure distributions will peak a considerable distance downstream of the "attachment" point. For example, for the ASTV case 2, the reattachment length is 0.15 while the pressure peaks at an x/d of about 0.8 and the heating rate at an x/d of 1.0. It is clear that the heating on the payload can be sharply reduced by keeping the payload short.

As previously mentioned with regard to the sphere benchmark case, the peak pressure in the rarefied wake does not correspond closely with a stagnation point as is the case with wakes at a high Reynolds number. The local flow is quite rarefied in the recirculation region with the mean-free-path being approximately equal to the reattachment length. In fact, the separation or recirculation which appears with the long time averaging of the molecular motion, where there are too few collisions for equilibrium to exist is really not a "separation" in the continuum sense, and the interpretation that this is a recirculation region stems from the continuum streamline concept. While this makes sense with respect to continuity (mass flow), it can give an erroneous impression of the actual local flow conditions. For example, consider a two-dimensional trailing edge problem with upper and lower streams expanding around the trailing corners and intersecting each other. In continuum flow, the two streams interact and turn to accommodate each other. In a very rarefied flow, the two streams may pass through each other with little or no interaction. The resulting streamline patterns from the two very different flows would look similar. The point being that, in addition to temperature and pressure, streamlines and consequently separation and reattachment do not have the same implication in rarefied flow that one is accustomed to in continuum flow.

4

REFERENCES

1. Bird, G.A.: "Molecular Gas Dynamics." Clarendon Press, Oxford.

2. Bird, G.A.: "Direct Simulation of Gas Flows at the Molecular Level." Communications in Applied Numerical Method, vol. 4, 1988, pp. 405–420.

3. Bird, G.A.: "Monte-Carlo Simulation in Engineering Context." Rarefied Gas Dynamics, vol. 74, Part I, edited by S.S. Fisher, AIAA, New York, 1981, pp. 239–255.

4. Shinn, J.L., Moss, J.N., and Simmonds, A.L.: "Viscous Shock-Layer Analysis for the Shuttle Windward Symmetry Plane With Surface Finite Catalytic Recombination Rates." Progress in Astronautics and Aeronautics: Entry Vehicle Heating and Thermal Protection Systems, edited by Bauer and Collicott, vol. 85, 1983, pp. 149–180.

5. Bird, G.A.: "The G2/A3 Program System Users Manual." Version 1.3, September 1988.

6. Muthoo, S.K., and Brundin, C.L.: "Near Wake Flow Field Measurements Behind Spheres in Low Reynolds Number Hypersonic Flow." Ninth Int. Sym. on RGD, 1:B, 10–1.

7. Dogra, V.K., Moss, J.N., Wilmoth, R.G., and Price, J.M.: "Hypersonic Rarefied Flow Past Spheres Including Wake Structure." AIAA 92-0495, 30th Aerospace Sciences Meeting and Exhibit, January 6–9, 1992.

8. Koppenwallner, G.: "The Drag of Simple Shaped Bodies in the Rarefied Hypersonic Flow Regime." AIAA-85-0998, AIAA 20th Thermophysics Conference, June 19–21, 1985.

9. NASA, Ames Research Center, NAS Technical Summaries, March 1988–February 1989.

Table 1. Freestream conditions for sphere calculations.

Case	V (m/s)	n	T (K)
1	721	0.4068×10^{22}	41.25
2	721	0.8137×10^{22}	41.25
3	721	0.2369×10^{23}	41.25
4	721	0.3353×10^{23}	41.25
5	721	0.5345×10^{23}	41.25
6	2,827	0.2935×10^{23}	22.10
7	2,827	0.6662×10^{23}	22.10

Table 2. Selected sphere freestream parameters.

Case	M	M	Re	Re_o	Kn	S
1	28.97	5.6	627.0	97.3	0.0134	4.69
2	28.97	5.6	1,254.0	194.5	0.0068	4.69
3	28.97	5.6	3,652.0	566.3	0.0023	4.69
4	28.97	5.6	5,169.0	801.6	0.0017	4.69
5	28.97	5.6	8,240.0	1,278.0	0.0010	4.69
6	28.97	30.0	33,058.0	565.0	0.0014	25.1
7	28.97	30.0	74,600.0	1,272.0	0.0006	25.1

Table 3. Molecular parameters.

Case	ω	T_{ref} (K)	$D_{N_2} (m \times 10^{10})$	$D_{O_2} (m \times 10^{10})$
1–5	0.9394	300.0	4.374	4.203
6–7	0.5560	1,000.0	3.405	3.265

Table 4. Freestream conditions for ASTV calculations.

Case	V (km/s)	n	T (K)	Mass Fractions		
				χ_{O_2}	χ_{N_2}	χ_O
1	10	0.1350×10^{21}	186.87	0.2408	0.7594	0.0000
2	10	0.4640×10^{20}	186.87	0.2408	0.7594	0.0000
3	10	0.1189×10^{20}	195.00	0.1824	0.7811	0.0365
4	10	0.2144×10^{19}	240.00	0.1228	0.7692	0.1080

Table 5. Selected ASTV freestream parameters.

Case	M	M	Re	Kn	S
1	28.970	36.5	5,183.0	0.0104	30.54
2	28.970	36.5	1,781.0	0.0302	30.54
3	28.299	35.24	430.0	0.1180	29.54
4	27.203	31.1	62.6	0.6548	26.11

(a) Nondimensional density, ρ/ρ_∞

(b) Nondimensional velocity, V/V_∞

(c) Nondimensional Temp, T/T_0
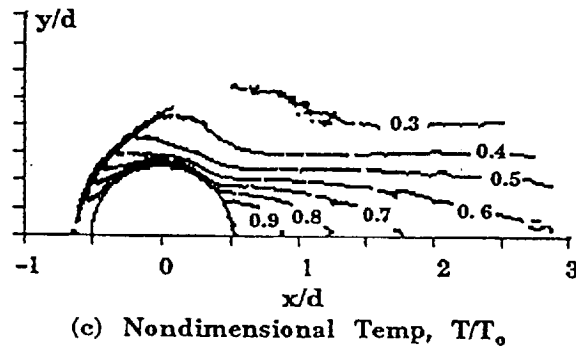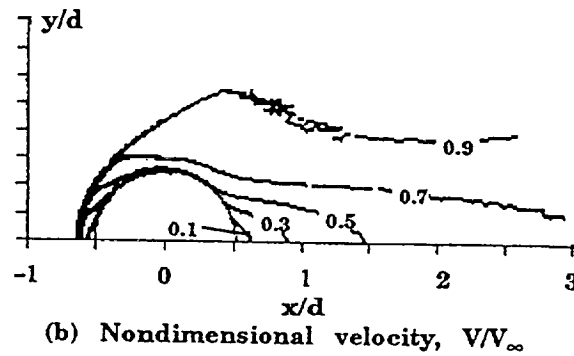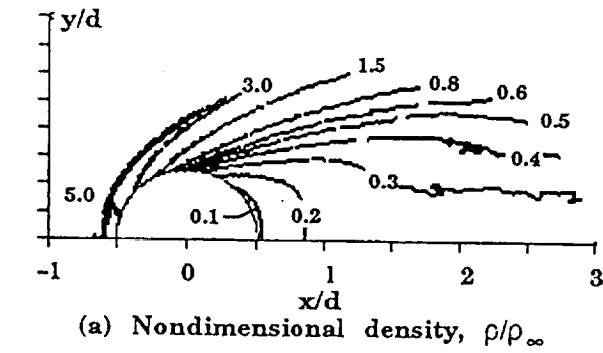
Figure 1. Selected variable contours about a sphere, case 2, $T_w/T_o = 1$.
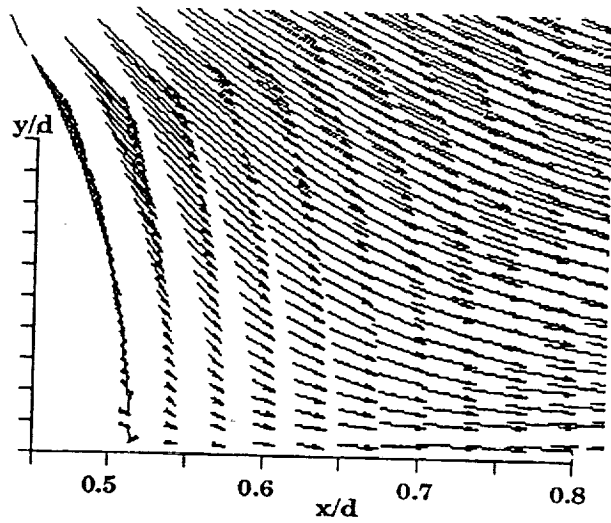
Figure 2. Flow vectors in near wake of a sphere, case 2, $T_w/T_o = 1$.

(a) Nondimensional density, ρ/ρ_∞

DSMC • , Experiment ◯ , Case 2, $T_w/T_o = 1$.

(b) Nondimensional velocity, V/V_∞

(c) Nondimensional Press, p/p_∞

(d) Nondimensional Temp, T/T_∞
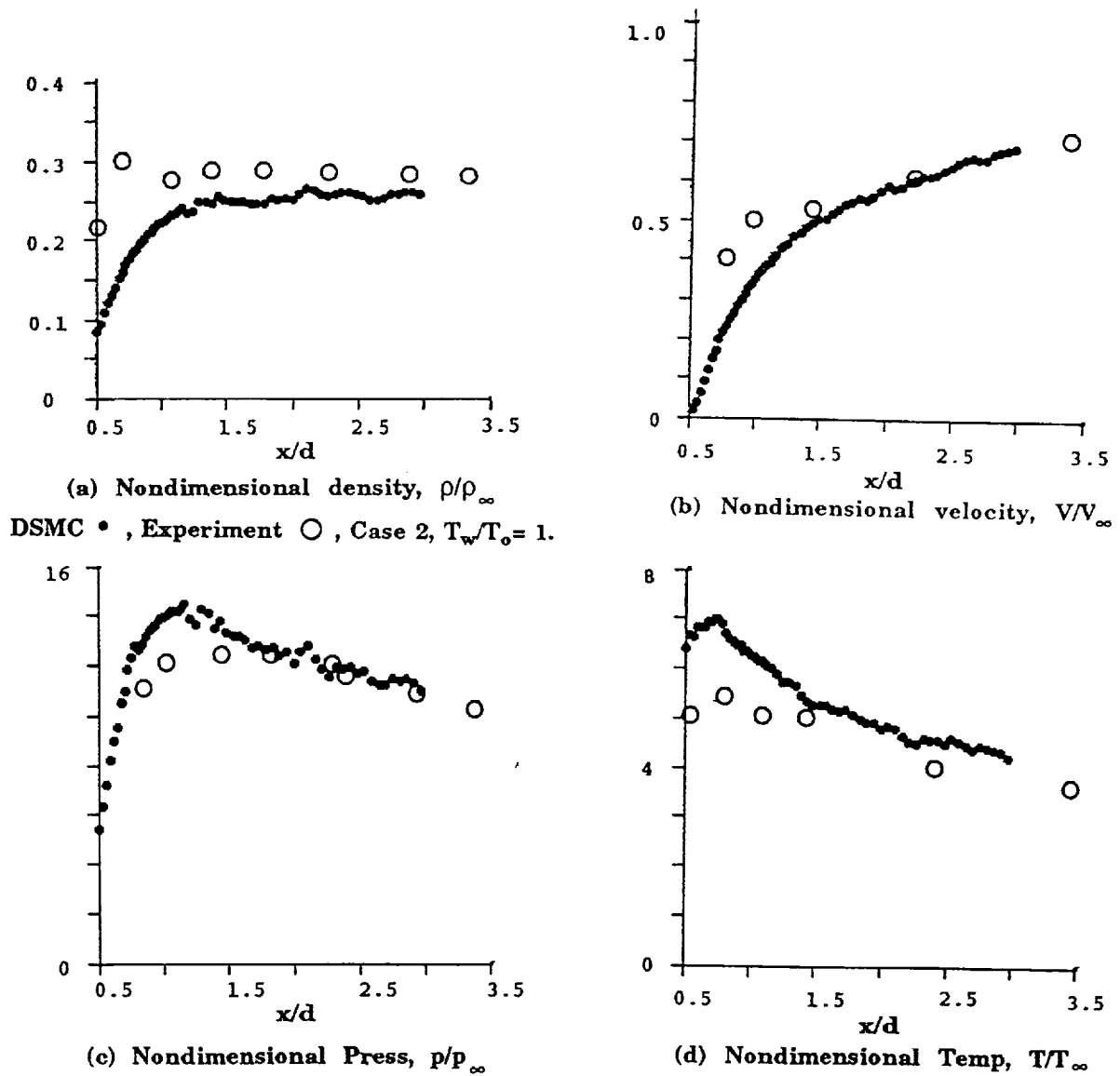
Figure 3. Comparison of selected variables along sphere wake centerline.

8

(a) Nondimensional density, ρ/ρ_∞

(b) Nondimensional velocity, V/V_∞

(c) Nondimensional Temp, T/T_0
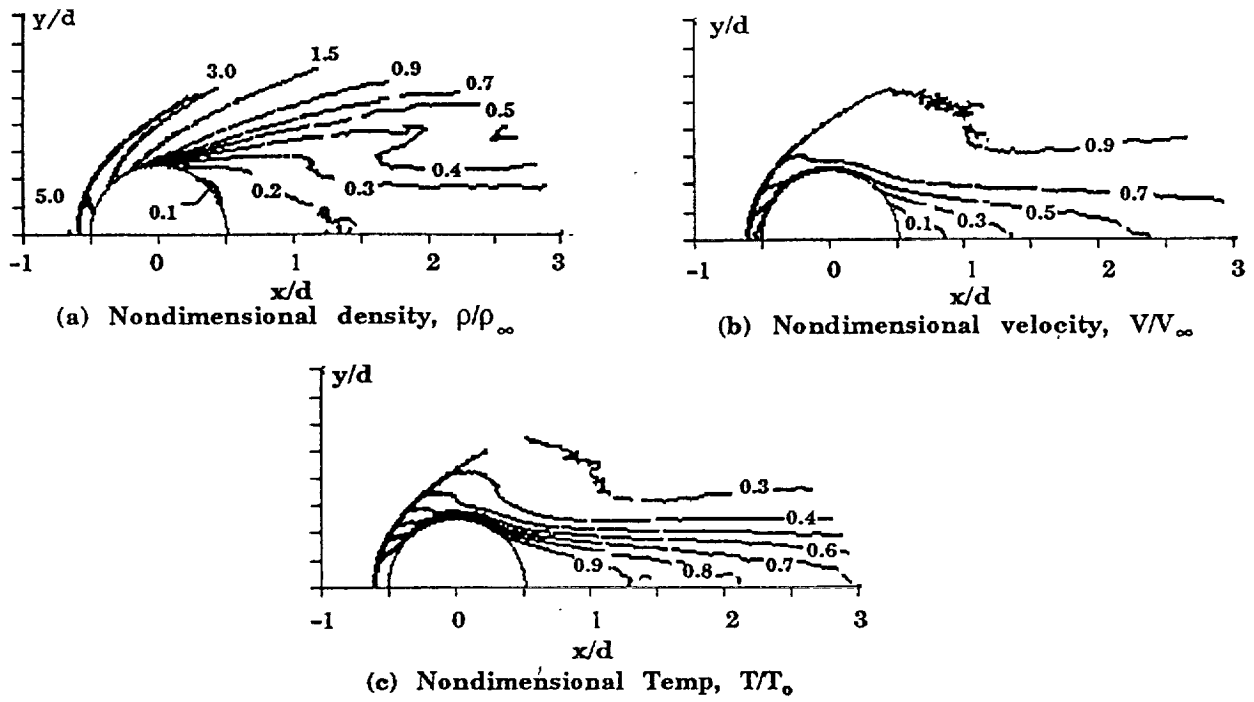
Figure 4. Selected variable contours about a sphere, case 4, $T_w/T_o = 1$.
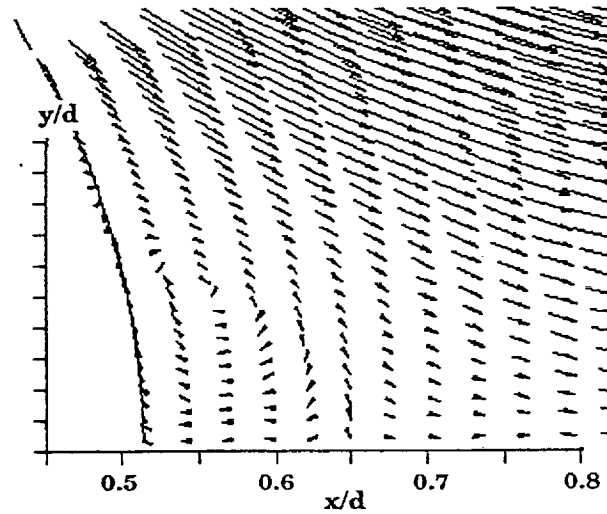
Figure 5. Flow vectors in a near wake of a sphere, case 4, $T_w/T_o = 1$.

●, M=5.6

■, M=30; Closed sym $T_w/T_o=1.0$; Open sym $T_w/T_o=0.1$
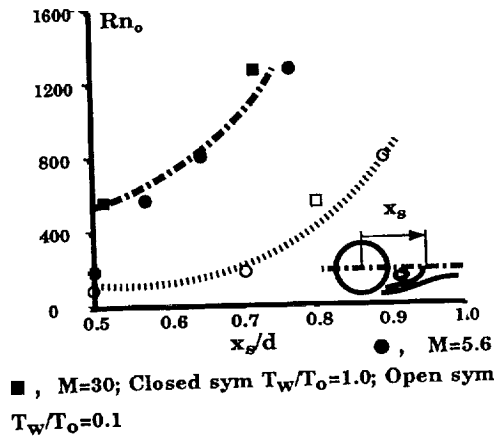
Figure 6. Extent of laminar flow separation behind a sphere from DSMC.
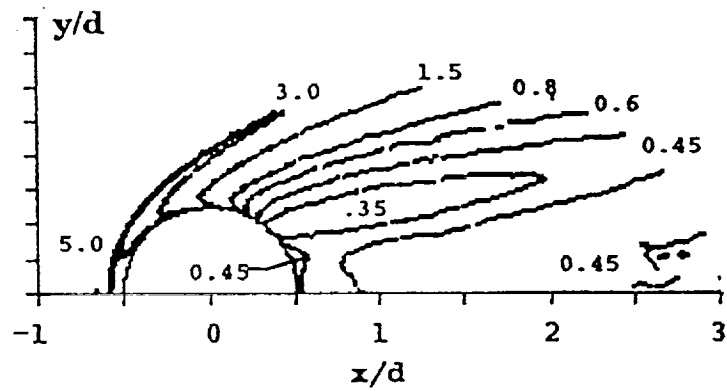
9

(a) Nondimensional density, ρ/ρ_∞
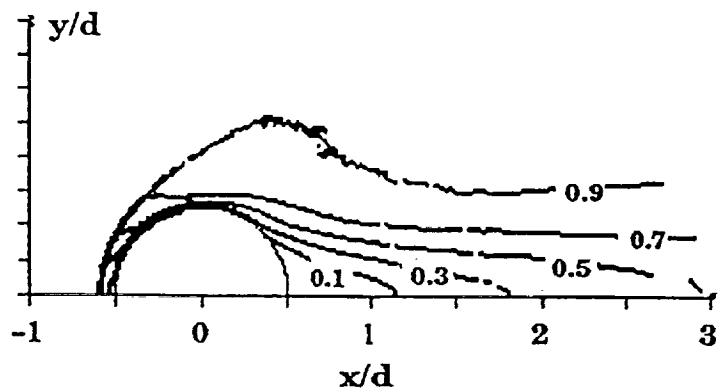
(b) Nondimensional Velocity, V/V_∞
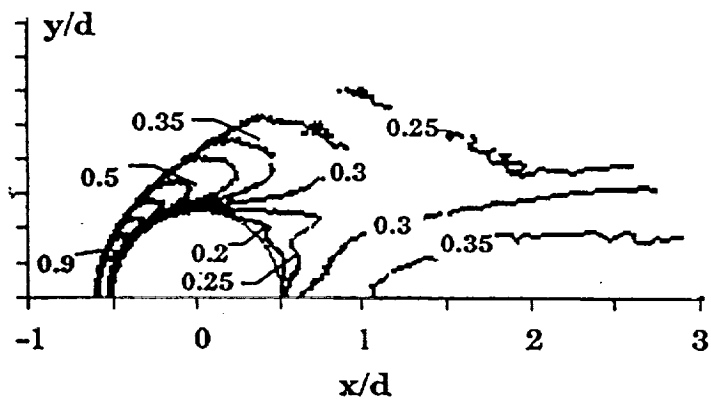
(c) Nondimensinal Temp, T/T_o

Figure 7. Selected variable contours about a sphere, case 4, $T_w/T_o = 0.1$.
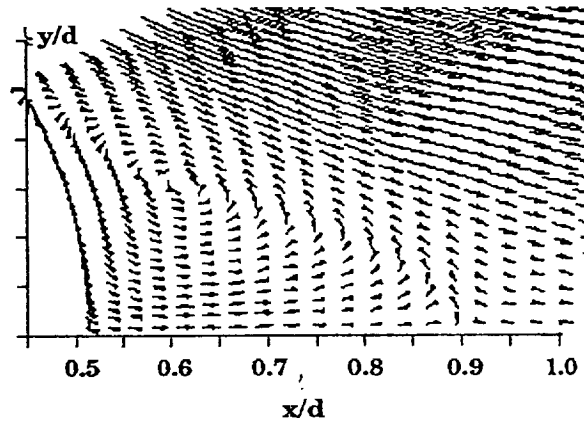
Figure 8. Flow vectors in near wake of a sphere, case 4, $T_w/T_o = 0.1$.
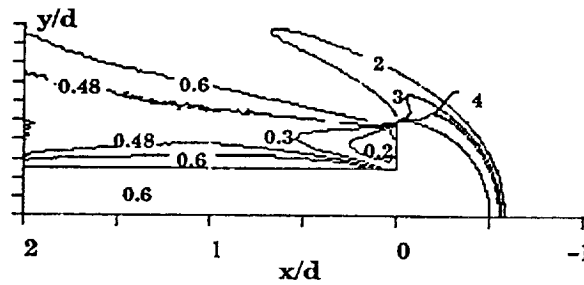
(a) Nondimensional density, ρ/ρ_∞
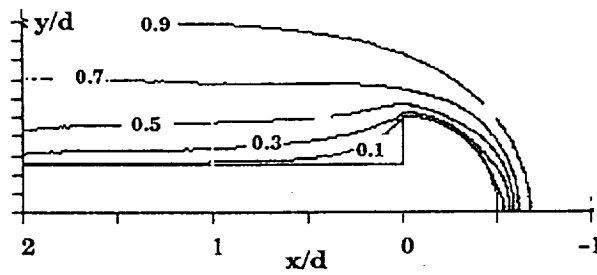
(b) Nondimensional velocity, V/V_∞
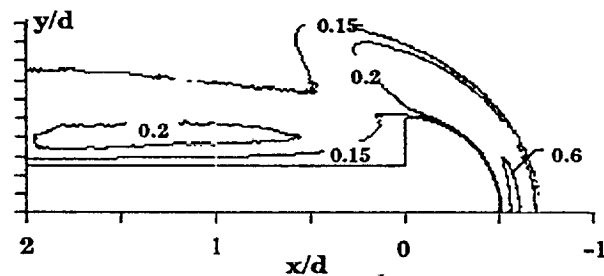
(c) Nondimensional Temp, T/T_o

Figure 9. Selected contours in an ASTV wake with diffuse B.C. on payload, case 2.

11
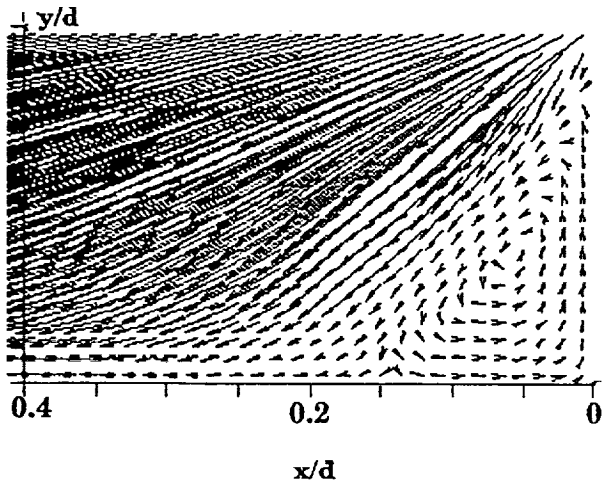
Figure 10. Flow vectors in an ASTV wake with diffuse B.C. on payload, case 2.
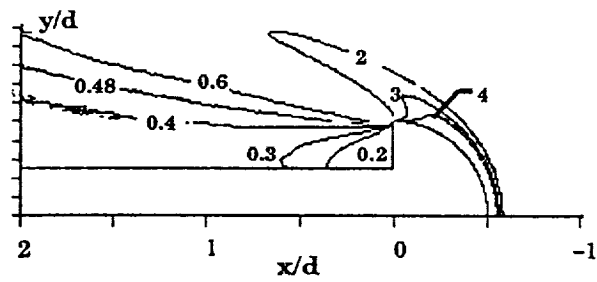
(a) Nondimensional density, ρ/ρ_∞
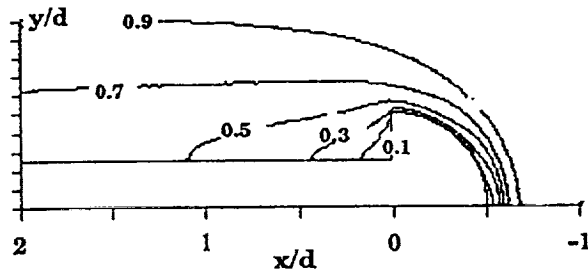
(b) Nondimensional velocity, V/V_∞
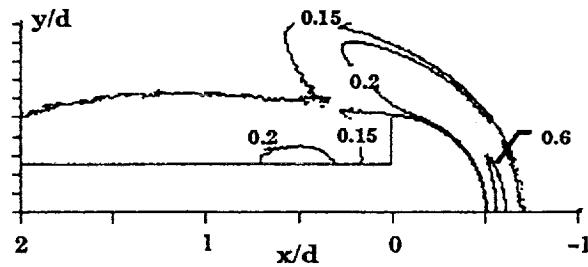
(c) Nondimensional Temp, T/T_0

Figure 11. Selected contours in an ASTV wake with specular B.C. on payload, case 2.
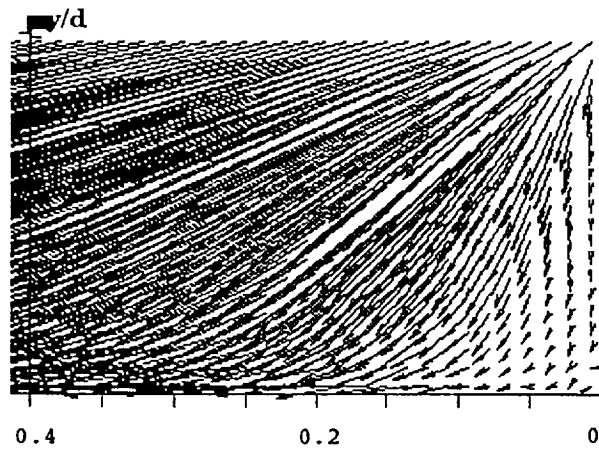
Figure 12. Flow vectors in an ASTV wake with specular B.C. on payload, case 2.
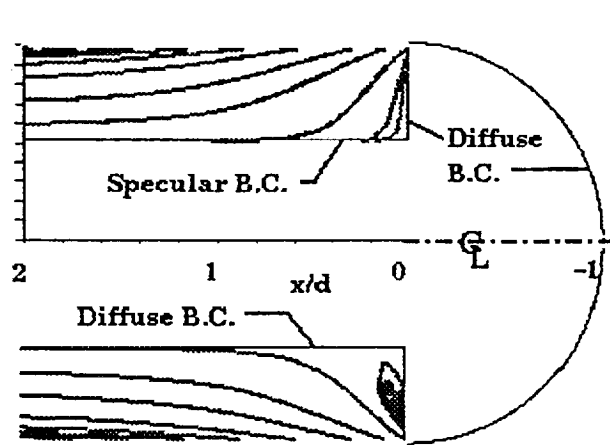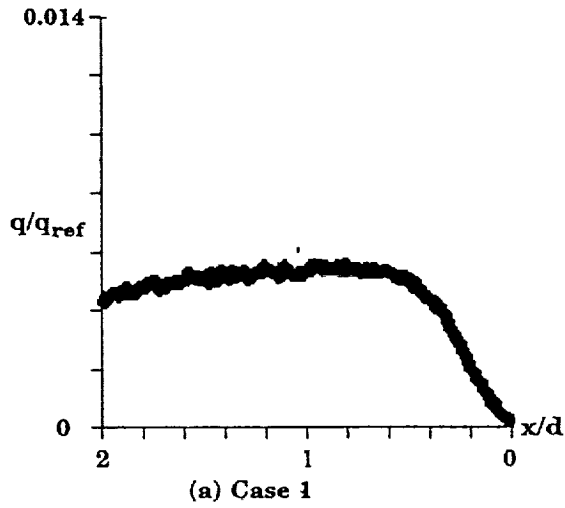

Figure 13. Streamlines in an ASTV wake, case 2.
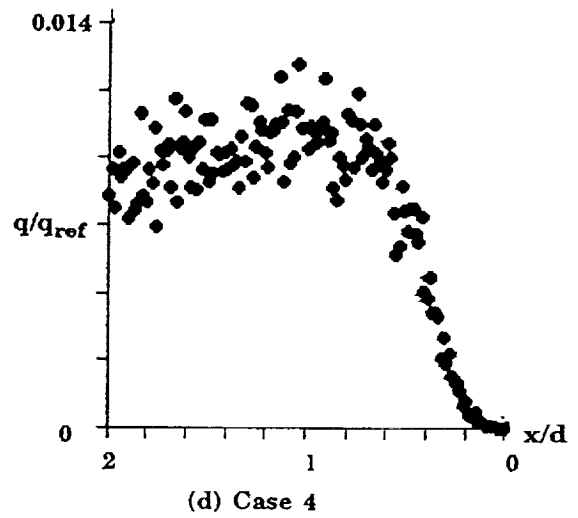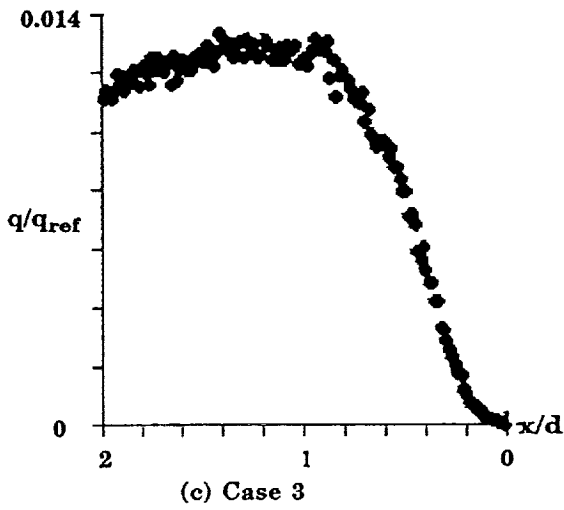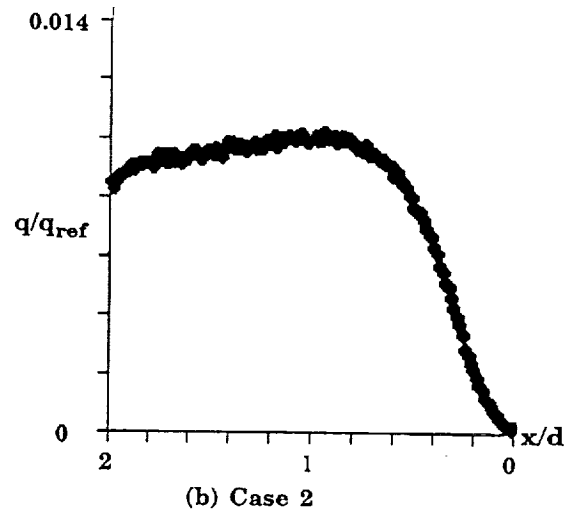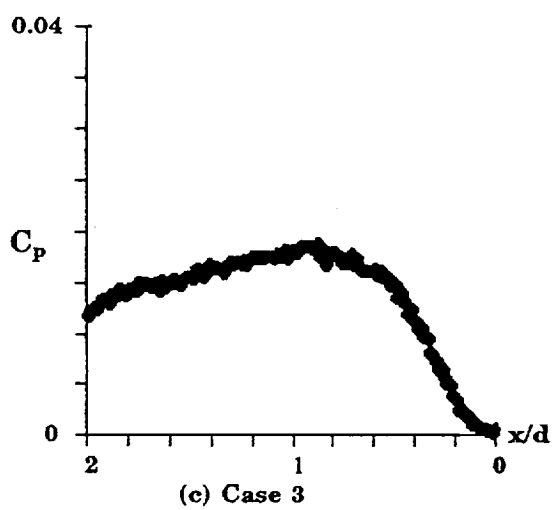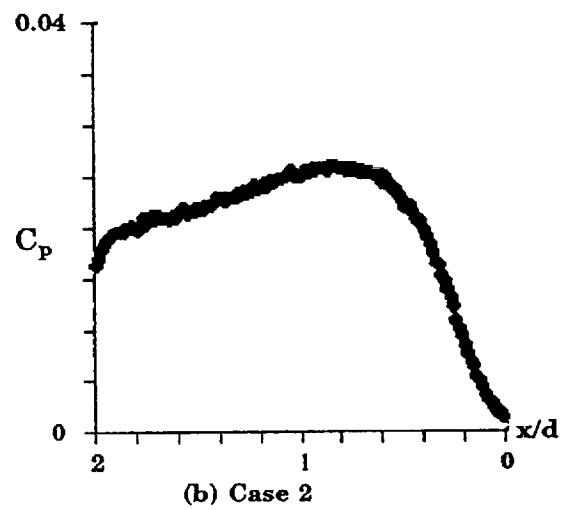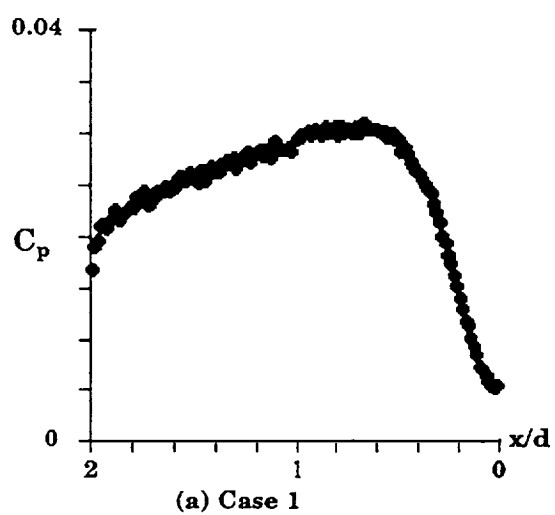
Figure 14. Nondimensional heating distribution along payload.
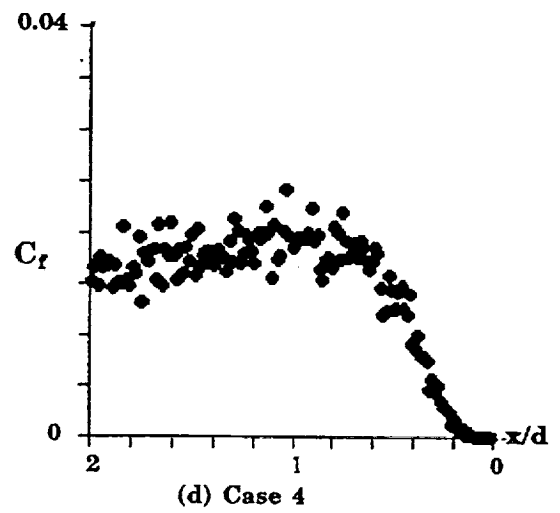
14
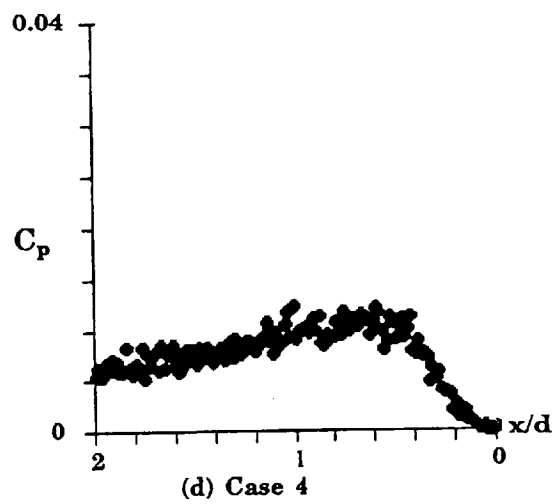
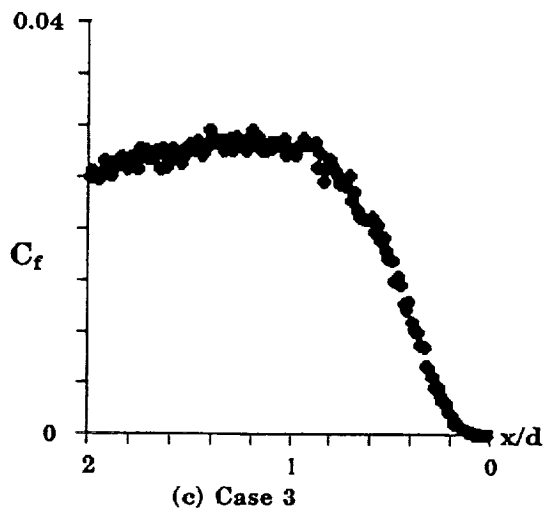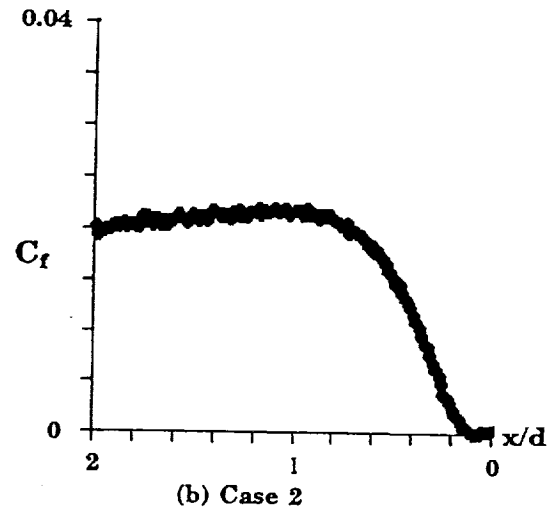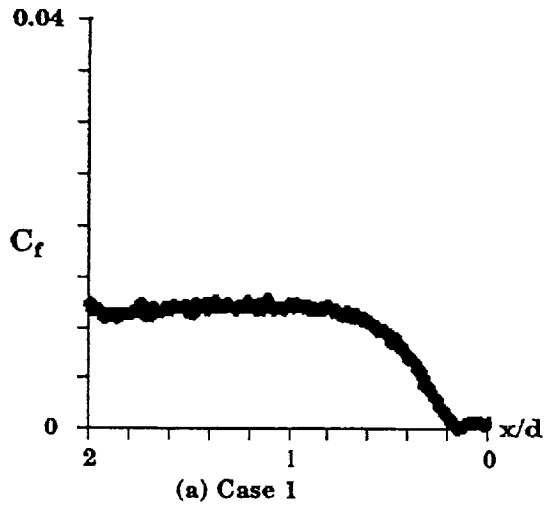Figure 15. Pressure coefficient distribution along payload.
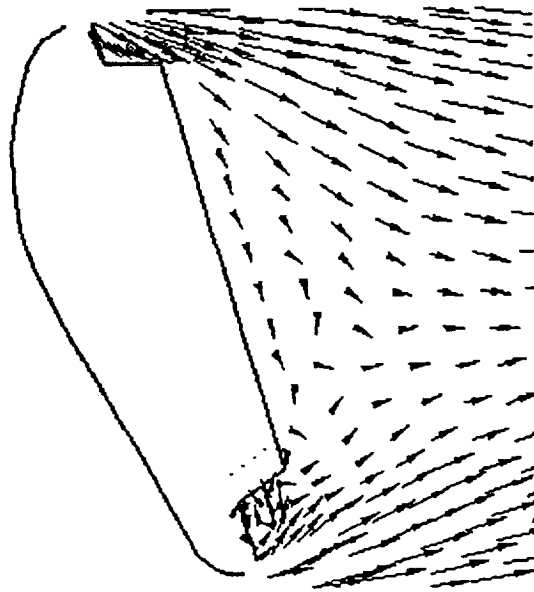
Figure 16. Skin friction coefficient distribution along payload.

Figure 17. Flow vectors in near wake of the AFE (altitude = 100 km, M = 30).

REPORT DOCUMENTATION PAGE

Public reporting burden for this collection of information is estimated to average 1 hour per response, including the time for reviewing instructions, searching existing data sources, gathering and maintaining the data needed, and completing and reviewing the collection of information. Send comments regarding this burden estimate or any other aspect of this collection of information, including suggestions for reducing this burden, to Washington Headquarters Services, Directorate for Information Operations and Reports, 1215 Jefferson Davis Highway, Suite 1204, Arlington, VA 22202-4302, and to the Office of Management and Budget, Paperwork Reduction Project (0704-0188), Washington, DC 20503.

1. AGENCY USE ONLY (Leave blank)	2. REPORT DATE January 1993	3. REPORT TYPE AND DATES COVERED Technical Paper

4. TITLE AND SUBTITLE

Hypersonic Rarefied Wake Characterization

5. FUNDING NUMBERS

6. AUTHOR(S)

E.B. Brewer

7. PERFORMING ORGANIZATION NAME(S) AND ADDRESS(ES)

George C. Marshall Space Flight Center
Marshall Space Flight Center, Alabama 35812

8. PERFORMING ORGANIZATION REPORT NUMBER

M-711

9. SPONSORING/MONITORING AGENCY NAME(S) AND ADDRESS(ES)

National Aeronautics and Space Administration
Washington, DC 20546

10. SPONSORING/MONITORING AGENCY REPORT NUMBER

NASA TP-3327

11. SUPPLEMENTARY NOTES

Prepared by Structures and Dynamics Laboratory, Science and Engineering Directorate.

12a. DISTRIBUTION/AVAILABILITY STATEMENT

Unclassified—Unlimited

Subject Category: 34

12b. DISTRIBUTION CODE

13. ABSTRACT (Maximum 200 words)

Results of a numerical study using the direct simulation Monte Carlo (DSMC) method are presented for hypersonic rarefied flow over an aeroassisted space transfer vehicle (ASTV). The emphasis of the study is the characterization of the near wake region which includes the ASTV payload. The study covered the transitional flow regime from near continuum to free molecular. Calculations show that the character of the near wake is significantly affected by the presence of the payload. Flow separation occurs when an afterbody is present throughout the transitional flow regime. In contrast, when no afterbody is present, no separation is observed until the flow approaches continuum.

14. SUBJECT TERMS

direct simulation Monte Carlo (DSMC), hypersonic, wake, transitional flow, aeroassisted space transfer vehicle (ASTV)

15. NUMBER OF PAGES
 28

16. PRICE CODE
 A03

17. SECURITY CLASSIFICATION OF REPORT Unclassified	18. SECURITY CLASSIFICATION OF THIS PAGE Unclassified	19. SECURITY CLASSIFICATION OF ABSTRACT Unclassified	20. LIMITATION OF ABSTRACT Unlimited